Bead milling disruption kinetics of microalgae: Process modeling, optimization and application to biomolecules recovery from Chlorella sorokiniana

Téné Rosine Zinkoné, Imma Gifuni, Laurence Lavenant, Jeremy Pruvost, Luc Marchal

Bead milling disruption kinetics of microalgae: Process modeling, optimization and application to biomolecules recovery from *Chlorella sorokiniana*

Téné Rosine Zinkoné[b], Imma Gifuni[a], Laurence Lavenant[c], Jérémy Pruvost[b], Luc Marchal[b,*]

[a] *Dipartimento di Ingegneria Chimica, dei Materiali e della Produzione Industriale, Università degli Studi di Napoli "Federico II", Piazzale Tecchio, 80, Naples, Italy*
[b] *GEPEA, UMR CNRS 6144, University of Nantes, 37 bd de l'Université, 44602 Saint Nazaire Cedex, France*
[c] *INRA, Centre de Nantes, rue de la Géraudière, 44000 Nantes, France*

Industrial development of microalgae biomass valorization relies on process optimization and controlled scale-up. Both need robust modeling: (i) for biomass production and (ii) for integrated processes in the downstream processing (DSP). Cell disruption and primary fractionation are key steps in DSP. In this study, a kinetic model, including microalgal cell size distribution, was developed for *Chlorella sorokiniana* disruption in continuous bead milling. Glass beads of 0.4 mm size at impeller tip velocity of 14 $m.s^{-1}$ were used as optimal conditions for efficient cell disruption. These conditions allowed faster disruption of big cells than small ones. A modified expression of the Stress Number, including cell size effect, was then proposed and validated.

Separation of starch, proteins and chlorophyll by mild centrifugation was studied as function of the disruption parameters. Low energy consumption conditions led to extreme comminution. An intermediate zone drew attention for allowing moderate energy consumption and efficient metabolites separation by centrifugation.

1. Introduction

Microalgae are considered as a sustainable alternative feedstock for different industrial fields: food, feed, fuels, bioactive molecules (Chisti, 2008; Draaisma et al., 2013; Wijffels et al., 2010). The challenges for industrial development are still numerous. For high yield and robust large-scale production, the biomass characterization and the modeling of growing conditions are required. After that, the downstream processing (DSP) has to be developed with the aim of valorization of different fractions for a cost-effective process (Asyraf Kassim et al., 2017; Chew et al., 2017; Moreno-Garcia et al., 2017). Downstream unit operations are harvesting, cell disruption, phase's separation, extraction and purification. The costs for DSP, using currently available technologies, represents more than 50% of the overall exploitation costs. Therefore, optimization, intensification and step reduction in this field, are the priority issues (Davis et al., 2011; Molina Grima et al., 2003).

For the recovery of both hydrophilic and hydrophobic microalgal compounds, the wet route processing (no preliminary drying) is the most adopted strategy, and it starts with the protein and polysaccharides release in an aqueous phase. The wet route reduces the process cost due to dewatering. In such a process scheme, the different fractions yield and purity are highly influenced by the method used for their release from the cells (Angles et al., 2017). In this sense, the cell disruption is a crucial step as well as other pretreatment operations in biorefinery schemes.

Mechanical cell disruption, in particular bead milling, is a promising technique for industrial scale application due to its efficiency of disruption and the commercially available devices at large scale (Günerken et al., 2015). The main drawbacks are the high energy demand, the heat production (cooling is necessary) and a complex product release in the lysate. Indeed, extreme bead milling disruption produces lysates, characterized by the production of very small cell debris and consequent molecular aggregations which are difficult to separate. Therefore, mild cell disruption conditions should be adjusted to minimize these drawbacks and to preserve the integrity of the released molecules (Phong et al., 2017). A modeling of the cell disruption mechanisms taking into account the bead milling operating conditions and the specificities of microalgae, is then necessary.

Several studies were addressed to the description of the process from the mathematical point of view in order to find the main parameters for the optimization. In particular, cell disruption kinetics was successfully described with a first order kinetics model by

* Corresponding author.
E-mail address: luc.marchal@univ-nantes.fr (L. Marchal).

Balasubramanian et al. (2011), Garrido et al. (1994) and Kwade and Schwedes (2007). This model was recently transposed from yeast to microalgae disruption (Montalescot et al., 2015; Postma et al., 2017).

Montalescot et al. (2015) used stress models coupled with the bead miller hydrodynamics modeling to describe cell disruption and the energy input as function of the process parameters. A critical stress intensity corresponding to the optimal parameters to balance efficient disruption and efficient energy use was identified.

Moreover, the comparison of the disruption behavior of different microalgae species (Montalescot et al., 2015; Postma et al., 2017) revealed that disruption kinetics in bead milling is strain-related. The differences between the strains were attributed to cell size, and to the composition and rigidity of cell membrane and cell wall. In non-synchronized cultures, microalgal cells are normally distributed in different size classes corresponding to different growth stages. The study of synchronized cultures (de Winter et al., 2013) proved that during growth phase cells become bigger and accumulate first pigments and proteins, and then energy storage metabolites such as lipids and starch until the division step. After division, cells are smaller with obviously lower product content. The rigidity of cell membrane is also reduced in big cells and easier disruption can be expected but no experimental evidence was reported yet. As cell composition and rigidity varies with their size, a possible prediction of the disruption kinetics according to cell size and to the process parameters should open the way for an effective optimization of the disruption process.

The aim of the present study is to identify a relation between the bead milling parameters and: I) the kinetics of disruption for different cell size classes; II) the purity for specific cell metabolite release. To this end, the first order kinetics model was evaluated for describing the cell disruption of each cell size classes. The effects of the operating parameters were studied. The stress model was modified and implemented for interpolation and extrapolation purposes. Mild centrifugation was then used to settle part of the non-soluble particles and to study the purity of biomolecules release in the water phase. Centrifugation conditions were chosen to ensure low energy investment and compatibility with low-cost and large-scale equipment. The partitioning of proteins, pigments and starch between pellet and supernatant was related to the bead milling parameters.

2. Materials and methods

2.1. Microalgal strain and culture

The microalgal strain used in this study was *Chlorella sorokiniana* Shihiraet Krauss strain (ACUF 318), provided by ACUF collection (http://www.acuf.net). The growth was performed in autotrophic conditions using modified BBM medium (Van Vooren et al., 2012). The culture was carried out in a flat panel photobioreactor (PBR) of 5 L characterized by a thickness of 3 cm and continuously illuminated on the front side by white light at 280 µmol.m^{-2}.s^{-1}. The PBR was operated in chemostat mode with a dilution rate of 0.4 d^{-1} in order to have every day the minimum amount of culture for disruption experiments, with constant and reproducible biomass conditions for each test. The microalgal culture, at steady state (concentration of 1 g.L^{-1}) was directly processed by bead milling without previous concentration step.

2.2. Bead milling disruption

Disruption experiments were performed in Dyno-mill multi lab from Willy A Bachofen AG (Muttenz, Switzerland). The bead milling was operated in pendulum mode as already described by (Montalescot et al., 2015). The temperature was maintained below 20 °C, the flow rate was set at 200 mL.min^{-1} and the filling ratio of the grinding media at 80%. Bead density (glass, zirconia), bead diameter (0.2–1.3 mm) and the impeller tip velocity (8–14 m.s^{-1}) were varied in order to test different stress intensities referred to the stress model.

Cell counting and cell size distribution were performed at process outlet, for each pass in the bead mill, using image analysis with the software ImageJ (1.50b, Wayne Rasband National Institutes of Health, USA). At steady state, (after 3 chamber's volumes) 10 mL of sample was collected. Cells were then fixed with 20 µmol of Lugol's iodine per mL of sample to enhance the contrast. The sample was placed in two Malassez counting plates and analyzed by a *Carl Zeiss* optical microscope equipped with an Axioscope A1 camera. 50 pictures were taken on the grided areas of the Malassez plates (25 pictures/plate). The camera settings were kept identical for each sample. The 50 images were treated simultaneously applying: a) a conversion to 8 bits images; b) a thresholding into white and black and particle analysis. The thresholding levels were calibrated to have a deviation lower than 10% with manual counts of 5 pictures picked randomly. For particle analysis, the ratio between pixels and real size was 4 pixels/µm. Particle size and shape were the criteria to differentiate non-disrupted cells from cell debris. For this purpose, the equivalent spherical diameter (D_{ESD}: diameter of an equivalent sphere which has the same area of projection as the particle) and the circularity (Circ: ratio between the particle perimeter and the perimeter of a sphere with the D_{ESD}) were used as filters to characterize size and shape:

$$D_{ESD} = 2 \times \sqrt{\frac{A}{\pi}} \tag{1}$$

$$Circ = 4 \times \frac{A}{\pi D_{ESD}} \tag{2}$$

with A the projection area of the particle.

To set the ranges of these filters, the size and the shape of intact cells at the steady state of the culture were analyzed. The cells sizes were between 2.5 and 8 µm with a mean circularity of 0.93. The ranges of the filters were chosen to select most of the non-disrupted cells in the lysates without counting cell debris. The selected ranges, were: $2.5 < D_{ESD} < 10$ µm and $Circ \geq 0.85$. The cell size distribution was divided into 0.5 µm wide size classes. The disruption rate were calculated for each pass using the following equations:

$$\eta_j(i) = 1 - \frac{N_j(i)}{N_0(i)} \tag{3}$$

$$\eta_j(i) = 1 - (1 - \eta_j(i))^j \tag{4}$$

$\eta_j(i)$: the disruption rate after the jth pass in the bead mill

$N_j(i)$ the number of non-disrupted cells of the size class i per mL of the lysate after the jth pass in the bead mill

$N_0(i)$ is the initial number of cells per mL of the class i in the microalgal suspension

2.3. Disruption modeling

2.3.1. Hydrodynamics and kinetics considerations

The cell disruption kinetics was modeled as a first order model for the overall population and for each size class. Concerning the process hydrodynamics, the two-continuously stirred tank reactors in series (CSTR) was used for the residence time distribution modeling as demonstrated in Montalescot et al (2015) for the same equipment.

The mass balance at the steady state of the continuous operation is written through (5) and (6) for the two CSTRs:

$$QN_0(i) = QN_1(i) + K_i N_1 \frac{V}{2} \tag{5}$$

$$QN_1(i) = QN_2(i) + K_i N_2 \frac{V}{2} \tag{6}$$

$N_0(i)$ (respectively $N_1(i)$) represents the number of cells of the class i per mL at the entrance of the first (respectively second) CSTR.

$N_1(i)$ (respectively $N_2(i)$) represents the number of cells of the class i per mL at the exit of the first (respectively second) CSTR.

V (mL) the free volume in the bead milling chamber.

Q (mL.min^{-1}) the flowrate of the microalgal suspension.

K_i (min^{-1}) the disruption kinetics constant for the size class *i*.

The combination of (5) and (6) allows the calculation of the disruption rate $\eta_1(i)$mod of the first pass using (7)

$$\eta_1(i)mod = 1-\left[\frac{1}{\left(1+\left(\frac{\tau_p}{2}\right)\times K_i\right)^2}\right] \quad (7)$$

with τ_p: the mean residence time equals to the ideal filling time (ratio between the free available volume in the grinding compartment and the volumetric flow rate) for a cascade of CSTRs in series.

The modeled $\eta_j(i)mod$ expressions for the following passes (j > 1) are deduced from $\eta_1(i)mod$ using (7).

The experimental $\eta_j(i)exp$ and modelled $\eta_j(i)mod$ were fitted by minimizing the cumulative square error defined in (8) to calculate the K_i.

$$\varepsilon^2 = \sum_{j=1}^{n}(\eta_j(i)exp-\eta_j(i)mod)^2 \quad (8)$$

2.3.2. Stress model

Kwade and Schwedes (Kwade, 1999a, 1999b; Kwade and Schwedes, 2007) developed stress models to describe the influence of the operating conditions in wet stirred media mills on the comminution of crystalline materials and yeast disruption. These models have been successfully extended to the disruption of microalgae by Montalescot et al. (2015) and Postma et al. (2017). The cell disruption rate during bead milling depends both on how frequently particles are stressed and how intense are the stressing events. In this sense, the effect of the bead milling operating parameters has been combined in 3 parameters:

- the stress intensity *SI* (J), the energy available at each stressing event for disruption;
- the stress number *SN* (-), the number of efficient stressing events (number of bead collisions with enough intensity to break particles);
- the specific energy E_m (J.kg^{-1}), amount of provided energy per product dry matter unit.

According to the stress model, when two of the three parameters are fixed independently of the corresponding set of operating parameters (impeller tip velocity, bead size and density, milling time…), the quality (disruption rate or product fineness) of the product during wet grinding is the same.

The real stress intensities and stress numbers distributions in the grinding chamber can only be obtained by complex numerical calculations combining the flow field and beads motion (Beinert et al., 2015; Blecher and Schwedes, 1996). Nevertheless, characteristic values of *SI* and *SN* based on the grinding mechanisms have been proposed and allowed the description of the influence of the bead milling operating parameters on the disruption efficiency.

The *SI* value has been expressed assuming that:

- the most intense and frequent mechanism of disruption is the result of the collision of beads due to high gradients of tangential velocity near the stirrer (Kwade, 1999a);
- only single particles are stressed between two colliding beads for particles larger than 1 µm in low solid concentration suspensions (when particles have enough freedom of motion) (Kwade, 1999a);
- the tangential velocity of the grinding media is proportional to the tip velocity of the impellers;
- the collision of bead to particle collisions are assimilated to elastic impacts (Becker et al., 2001) and the elasticity of the feed material is much smaller than that of the grinding media in cases of deagglomeration, cell disintegration and grinding of weak or medium hard crystalline materials (Kwade and Schwedes, 2002).

Therefore, the maximal stress energy available for disruption is proportional to the maximal kinetic energy of the grinding media.

$$SI_{max} \propto SE_B = \rho_B \cdot d_B^3 \cdot v^2 \quad (9)$$

with ρ_B (kg.m^{-3}), d_B (m), SE_B (J), the density, the diameter and the stress energy of the beads respectively and v (m.s^{-1}) the tip velocity of the impellers.

SN was assumed to be proportional to the number of contacts N_c (−) and the probability that a particle is sufficiently stressed during one stressing event P_s (−).

$$SN = N_c \cdot P_s \quad (10)$$

where $N_c \propto n.\ t.\ N_B$, n the number of stirrer revolutions per second, t the milling time and N_B the number of beads.

Kula and Schütte (1987) and Schwedes and Bunge (1992) showed that for microorganisms disintegration shear forces of the fluid between two colliding beads are sufficient for disruption and then that P_s is proportional to d_B^2.

Combining all these hypotheses, *SN* should be expressed as:

$$SN \propto \varphi\,(1-\varepsilon)\cdot\frac{n.\ t}{d_B} \quad (11)$$

ε (−) the bulk porosity of the beads, φ (−) the filling rate of the mill chamber, n (s^{-1}) the number of revolutions of the impeller per second.

The number of stress is commonly reported to the number of particles which is a parameter that decreases in the course of the process. Here the expression of *SN* represents the total number of stress.

In the present study, the disruption behavior is detailed for each size class of cells and the effect of cell size was included in the *SN* definition. Two expressions for *SN* were compared:

$$SN_1 = SF_1.\ t\,\alpha\,\zeta.\ n.\ t\frac{d_\mu}{d_B}\ with\ SF_1\,\alpha\,\zeta.\ n.\ \frac{d_\mu}{d_B} \quad (12)$$

$$SN_2 = SF_2.\ t\,\alpha\,\zeta.\ n.\ t\left(\frac{d_\mu}{d_B}\right)^3\ with\ SF_2\,\alpha\,\zeta.\ n.\ \left(\frac{d_\mu}{d_B}\right)^3 \quad (13)$$

$$\text{and}\ \zeta = \varphi.\ (1-\varepsilon) \quad (14)$$

In SN_1 the hypothesis that P_s is proportional to d_B^2 is maintained whereas for SN_2 implies that at any media contact a cell is disrupted ($P_S = 1$). d_μ and ${d_\mu}^3$ respectively are implemented in the definitions to describe the effect of cell size with dimensionless expressions. $SNi_1(0.9)$ and $SNi_2(0.9)$ respectively are the required number of stress events to reach 90% of disruption in the size class *i*. The required residence time to reach 90% $t_i(0.9)$ that includes hydrodynamics and kinetics modeling was calculated with (15) as a function of the kinetic constants K_i (from experiments).

$$t_i(0.9) = \frac{2}{K_i}\cdot\left(\sqrt{\frac{1}{1-0.9}}-1\right) \quad (15)$$

SI is the specific energy consumed at each stress event and consequently the product *SI*. *SN* is proportional to the treatment specific energy E_m (J.kg^{-1}). The proportionality factor is constant here due to the constant dry weight of the biomass (1 g.L^{-1}) used in the different disruption tests.

$$E_m \propto SI.\ SN \quad (16)$$

2.4. Centrifugation

The microalgal lysate generated by bead milling was centrifuged before carrying out the analysis of the released products. Centrifugation parameters were selected in order to ensure the efficient settling of

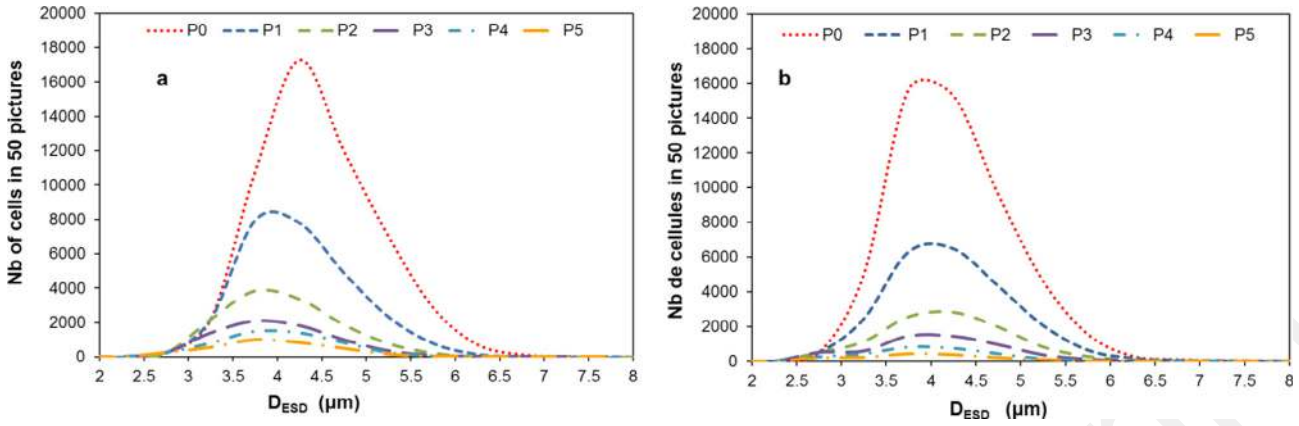

Fig. 1. *Chlorella sorokiniana* cells size distribution (number of cells at constant volume in each size class between 2 and 8 µm) during bead milling – P0: initial distribution – P1: 1st pass (t = 1.3 min) – P2: 2nd pass (t = 2.6 min) – etc. a) 0.375 mm glass beads and b) 0.2 mm zirconia beads at 10 m.s^{-1}.

dense and insoluble particles (such as starch) and minimum energy consumption. Mild centrifugation at 2500*g* was selected as optimal speed for low cost large-scale applications. The time necessary to settle starch granules (dense and insoluble) was calculated according to:

$$t = \frac{9H\eta_L}{2(\rho_P-\rho_L)r_P{}^2 g} \quad (17)$$

with t the time to achieve the starch settling (s), H the radial movement covered by the particles (m), η_L the lysate viscosity (Pa.s) ρ_P and ρ_L the densities of the starch particles and the density of the lysate respectively (kg.m^{-3}), r_P the mean diameter of microalgal starch granules; g the centrifugal acceleration (m.s^{-2}). The microalgal lysate was assumed to have physical properties close to water since it was characterized by low cell concentration (Montalescot et al., 2015; Souliès et al., 2013). The properties of the microalgal starch granules were previously reported in Gifuni et al. (2017). The calculated time was 3 min, for the settling of starch granules suspended in 3 mL of lysate.

2.5. Analysis of the recovered products

After disruption and centrifugation, two fractions were obtained: pellet and supernatant. The dry matter, starch, proteins and pigments were quantified in the two fractions.

The dry matter in the pellet was measured by weighting the pellet after drying at 100 °C for 24 h. The dry weight of the total biomass was measured by filtering a known amount of culture by cellulose filter, then dried at 100 °C for 24 h and weighted. The dry matter released in the supernatant was calculated as difference from the total dry weight of the biomass.

The starch concentration was assayed in the pellet by Total Starch Kit by Megazyme (Wicklow, Ireland). Proteins concentration was assayed in the supernatant by BCA Protein Assay Kit (Thermo Scientific). Pigments concentration was measured in the pellet by spectrophotometric quantification after methanol extraction (Kandilian et al., 2016).

The recovery was defined as the ratio between the metabolite quantity released in the pellet or the supernatant and the initial quantity in the crude biomass. The initial composition in the biomass was obtained as following:

- for the starch: quantity recovered in the pellet after two 270 MPa passes in high pressure disrupter (CellD, Constant System) at centrifugation at 3000*g* during 5 min;
- for the proteins: concentration expressed as BSA_{eq} in the supernatant after two 270 MPa passes in high pressure disrupter and centrifugation at 3000*g* for 5 min;
- for the pigments: methanol extraction on the intact cells after centrifugation.

The product yield (Y) was defined as the ratio between the mass of the product (m_α) in the recovery fraction (pellet for starch, supernatant for proteins and pigments) and the total mass of the product α in the initial biomass (M_α):

$$Y_\alpha = \frac{m_f^\alpha}{M_\alpha} \quad (18)$$

The purity (P^α) was defined as the ratio between the mass of the product α in the recovery fraction (m_f^α) and the total mass of the fraction (m_f).

$$P^\alpha = \frac{m_f^\alpha}{m_f} \quad (19)$$

3. Results and discussion

3.1. Biomass composition

C. sorokiniana concentration at the PBR outlet was 1.0 g.L^{-1}. The production was maintained in a steady state with constant irradiation and dilution rate.

At the steady state the biomass composition was constant over the time. In particular, the protein content was 35%, the starch content was 7–8%, the chlorophyll was 2–3%. The remaining fraction represented 55%. All the percentages were calculated based on 100 g of biomass dry weight.

3.2. Evolution of the size distribution during bead milling

For each experimental condition, the size distribution of the cells in the lysate has been followed in the course of the process time. Fig. 1 shows the evolution of the size distribution with 0.375 mm glass beads at 10 m.s^{-1} and with 0.2 mm zirconia beads at 14 m.s^{-1}. The culture of *Chlorella sorokiniana* had cell sizes ranging between 2.5 µm and 7.5 µm with a mean diameter D_{ESD} of 4.5 µm ± 0.2 µm and a standard deviation of 0.7 µm. Using 0.375 mm glass beads at 10 m.s^{-1} (Fig. 1.a), the size distribution slightly shifted to the left after the first pass. Big cells where disrupted more efficiently than the small ones. However, no similar trend was observed with the 0.2 mm zirconia beads at 14 m.s^{-1} (Fig. 1.b). Cell disruption kinetics was obtained by modeling the cell disruption rate for each size class as a function of time, taking into account the RTD (Residence Time Distribution) in the process.

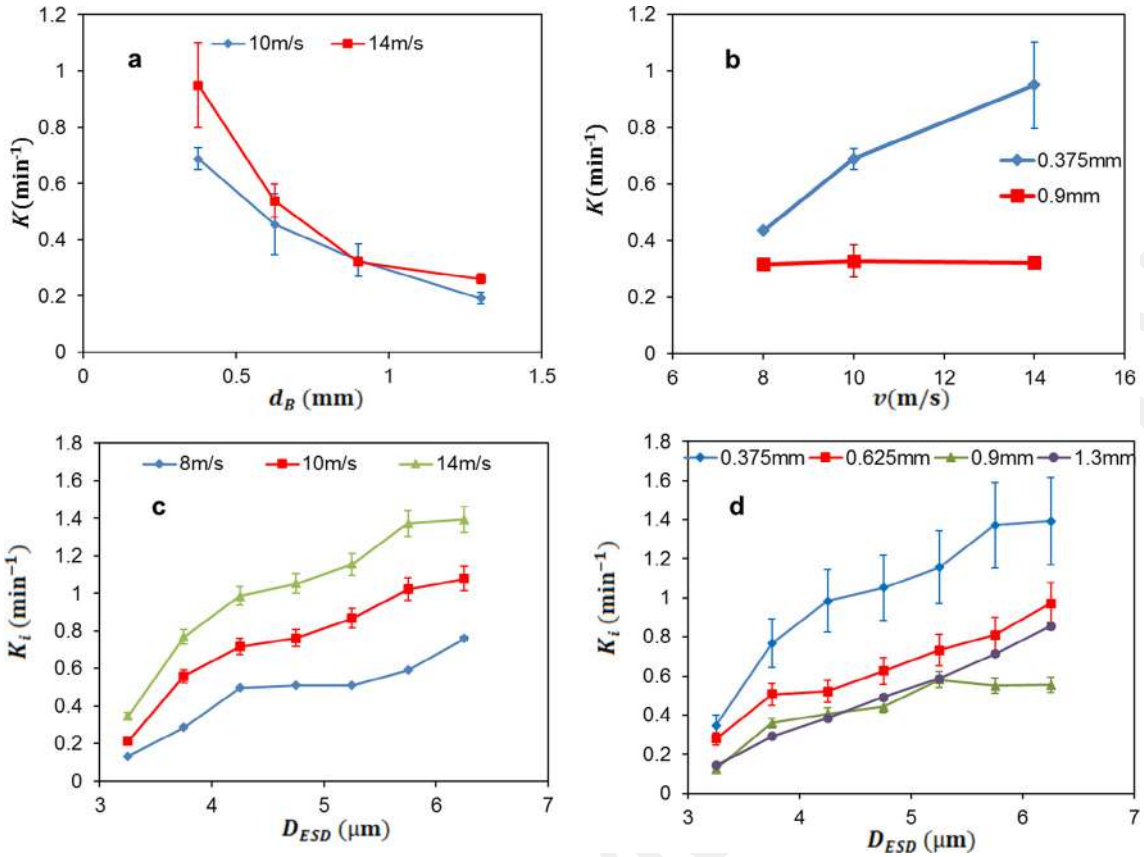

Fig. 2. Bead milling parameters effects on disruption kinetics – a) beads size effect on the overall kinetic constant K – b) Impeller tip velocity effect on the overall kinetic constant K – c) Disruption kinetic constants K_i according to the cell size for 8, 10 and 14 m.s^{-1} (0.375 mm glass beads) – d) Disruption kinetic constants K_i according to the cell size for 0.375, 0.625, 0.900 and 1.30 mm glass beads (14 m.s^{-1}).

3.3. Effect of bead size and agitation speed on the overall disruption kinetics

The effect of bead size and agitation speed on disruption kinetics is presented in Fig. 2. Due to an important counting uncertainty for extremely small and big cells (size classes with the lowest cell number), the calculation of disruption kinetics constants was restricted to 3 µm–6.5 µm. In Fig. 2.a, the disruption kinetics coefficient clearly decreased as the bead size increased. The 0.375 mm beads allowed three times higher K values than 1.3 mm beads. In Fig. 2.b, the impeller tip velocity also improved the disruption kinetics, but only for small beads whereas no significant improvement was observed for bigger beads (over 0.9 mm). Using smaller beads at a constant filling ratio results in higher beads number. The efficiency of small beads and high velocities can be explained by the fact that both conditions increase the stress frequency (Kwade and Schwedes, 2007).

3.4. Effect of cell size on the disruption kinetics

The higher resistance of small microalgae cells to bead milling disruption was previously reported by Montalescot et al. (2015) about two strains of spherical shape: *N. oculata* (3 µm mean diameter) and *P. cruentum* (4 µm-9 µm). Three times more mechanical energy was necessary for *N. oculata* to reach the same disruption level than *P. cruentum*. However, since the cell membrane and cell wall composition were different for the two strains, the robustness of *N. oculata* couldn't be attributed only to cell size.

Fig. 2c and d, show that the disruption kinetics (using glass beads) increased with cell size regardless of the impeller tip velocity or the bead diameter. Big cells of *C. sorokiniana* appeared to be more sensitive to the mechanical bead milling treatment.

The difference between big and small cells was accentuated by increasing the circumferential velocity of the impellers (Fig. 2.c). The difference was enhanced when 0.375 mm glass beads and 14 m.s^{-1} velocity are used. In these conditions, the kinetics constants value for 6.25 µm cells was 4 time higher (1.37 min^{-1}) than for 3.25 µm cells (0.35 min^{-1}). For example, in these conditions, for a 1 min of treatment, 75% of 6 µm cells were disrupted while, 70% of 3 µm cells remained intact. Such a behavior revealed the possibility to target bigger cells to recover metabolites that are preferentially accumulated in big cells. For *Chlorella sorokiniana*, the optimal conditions for efficient disruption were ~0.4 mm glass beads at 14 m.s^{-1} impeller tip velocity. As previously mentioned, the optimal conditions are strain dependent because of the different cell wall rigidity and composition, and the mean cell size. Optimization studies should be carried out for each adopted strain. Besides, this study aimed to provide a modeling tool for the selection of the bead milling parameters as function of a target cell size, responsible of specific product accumulation.

3.5. Stress model applied to each size class

3.5.1. Model validation

As mentioned in Section 2.3.2 two expressions for SN are proposed and compared. SN_1 (0.9) and SN_2 (0.9), defined in Eqs. (12) and (13), were calculated at t (0.9). t (0.9) is the treatment time necessary to reach 90% of disruption (16). In Fig. 3.a, SN_1 (0.9) values for the small cells were slightly higher than those of the big cells in the 10^{-5}–10^{-3} J SI range. In Fig. 3.b, the SN_2 (0.9) values are not correlated to the cell size as expected from the results of Section 3.4. SN_2 definition does not reflect the longer time needed by small cells, for a given value of SI (corresponding to a set of experimental conditions). Therefore, the definition SN_1 was selected for further analysis of the disruption behavior according to the cell size distribution.

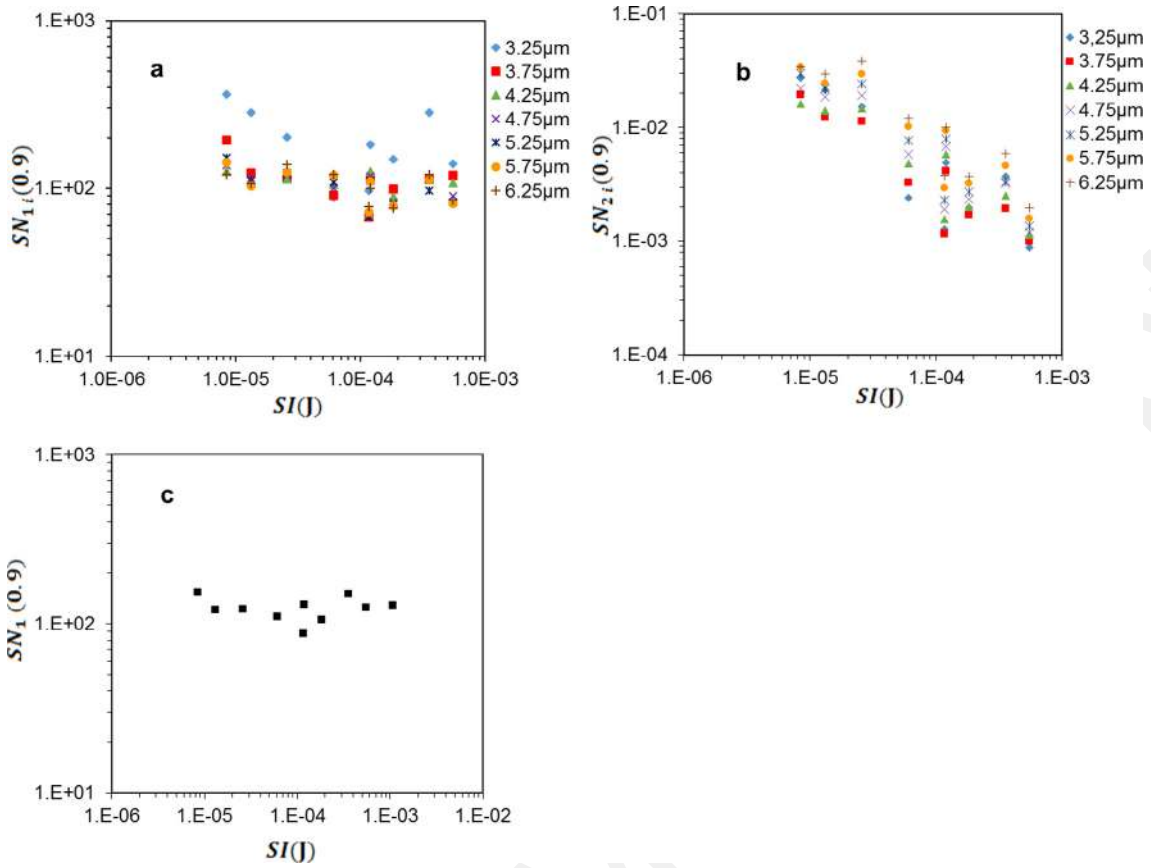

Fig. 3. Comparison of SN_1 (0.9) and SN_2 (0.9) for 90% disruption rate prediction according to the stress intensity *SI* (J) and the microalgal cell size – a) SNi_1(0.9) and b) SNi_2 ((0.9) – c) SN_1 (0.9) applied to the whole population as a function of SI value.

In Fig. 3.a, all the SN_1 (0.9) values calculated were around 10^2, except for the smaller cells (3.25 µm). Montalescot et al. (2015) found two zones in the *SI*/*SN* diagram: (i) for SI below the critical value, the *SN* (0.9) decreases when *SI* increases and (ii) after the critical value no further decrease was observed and *SN* (0.9) is quite constant. Considering the different size classes, for the small cells (3.25 µm) the *SN* value is the highest and it decreased with the *SI*, until a critical SI value around 2.10^{-5} J. For bigger cells, no critical value of SN_1 (0.9) was observed: all applied stress intensities were already higher than the critical one. In fact, Schwedes and Bunge (1992) already experienced higher stress intensities than the critical SI of yeast cells, when big glass beads were used.

In Fig. 3.c, considering the whole population, no significant effect of the *SI* on *SN*(90) was observed. The stress intensities tested were higher than the mean critical intensity required for *C. sorokiniana* cell disruption. In such conditions, the increase of the stress intensity does not reduce the required number of stress events to reach a given disruption rate, but it increases the energy consumption. For an optimal energy use, the bead milling should be operated around the critical *SI* value. In this study, the critical value was not properly detected, probably because it was lower than 2.10^{-5} J (the lowest *SI* here considered, Fig. 5).

3.5.2. *Prediction of the disruption kinetics*

The analysis of the disruption kinetics results of the different size classes, highlighted a correlation to the stress frequency, *SF*. In Fig. 4, the disruption kinetic constants for the various cell sizes (K_i) and for the overall population (K) are presented as function of SF_1. Except for

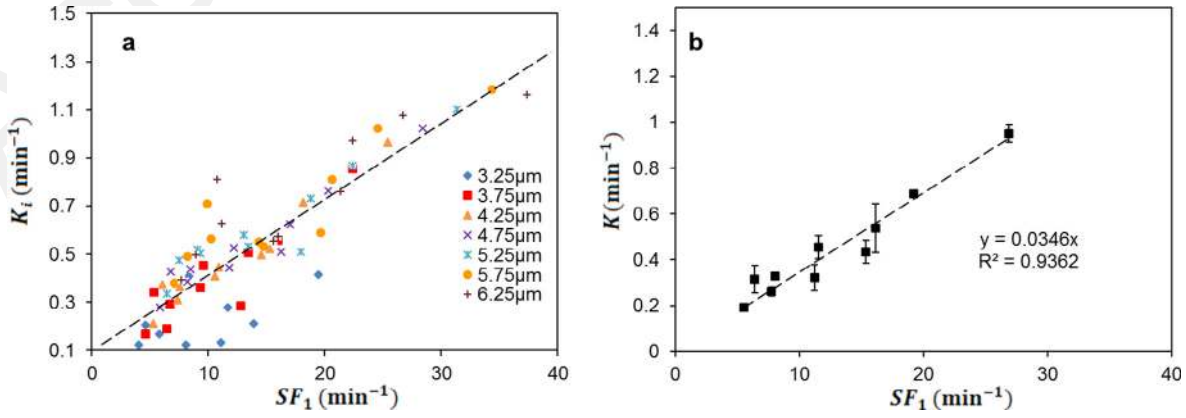

Fig. 4. Correlation between the disruption kinetic constants and the stress frequency SF_1 (s-1) – a) K_i for each size classes – b) K for the overall population.

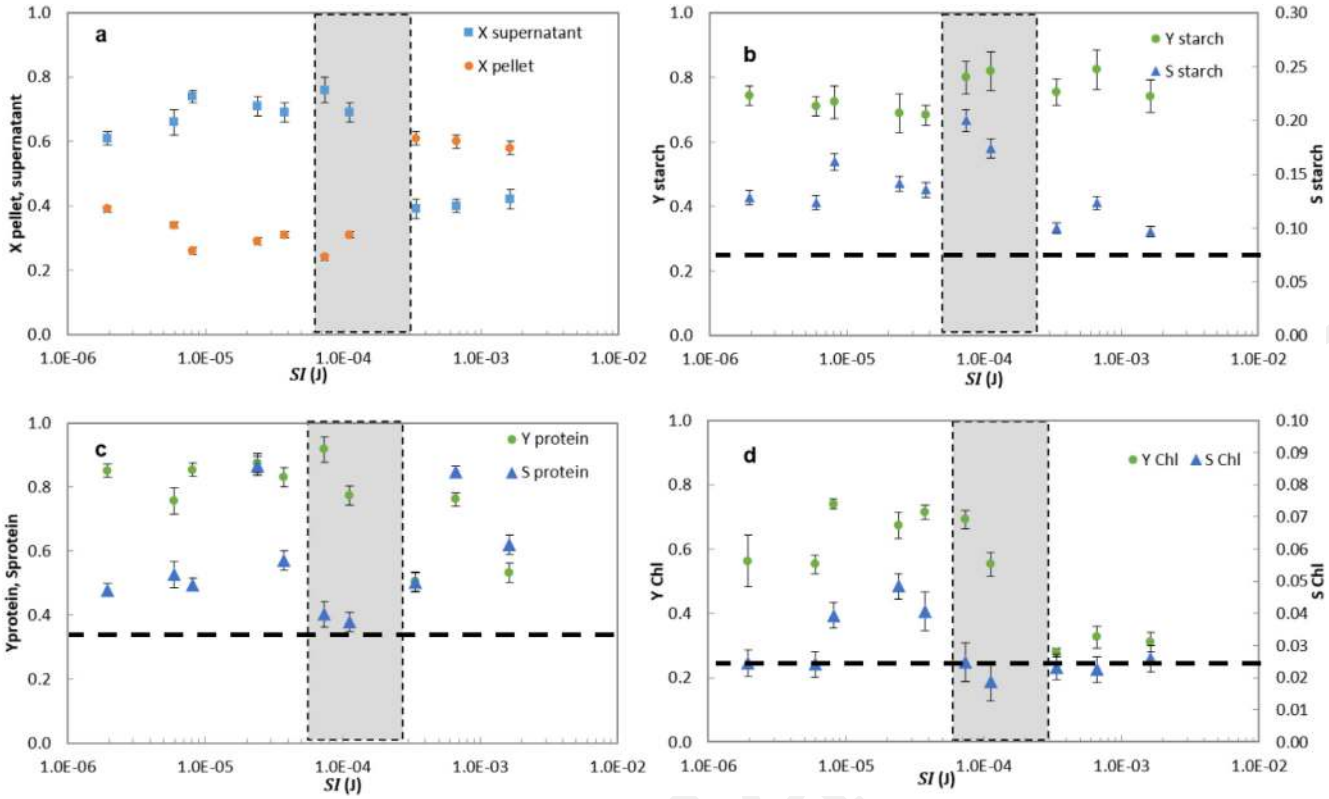

Fig. 5. Supernatant and pellet distribution of different products according to the *SI* value – a) dry matter recovery – b) starch yield and purity in the pellet – c) protein yield and purity in the supernatant – d) chlorophyll yield and purity in the supernatant – dashed lines correspond to initial biomass composition.

3.25 µm cells that had a slower disruption, all the other size classes followed the same trend of K_i proportional to the SF_1 value. The mean disruption kinetic constant K can be successfully predicted from SF_1 values. For *Chlorella sorokiniana,* it is a linear function of the stress frequency with $K = 0.035$. SF (K in min^{-1} and SF in min^{-1}).

3.5.3. Prediction of metabolites recovery as function of the energy consumption

The amount of metabolites recovered for different bead milling conditions was quantified. The recovery was referred to the selected centrifuge parameters calculated in the Section 2.4.

In Fig. 5, the partitioning of dry matter, starch, protein and chlorophyll between pellet and supernatant is shown as a function of the SI value. In all conditions, 90% of cell disruption was reached. In Fig. 5.a, the recovery of the dry matter in pellet and supernatant is shown; in Fig. 5b, c and d, the yield and the purity of starch recovery in the pellet, proteins and chlorophyll recovery in the supernatant are presented. A clear behaviour appeared for all the products:

- Below a *SI* range (1.10^{-5}–5.10^{-4} J), corresponding to the grey zone in Fig. 5, most of the dry matter (around 70%) still resides in the supernatant after the mild centrifugation. It resulted in high protein recovery in the supernatant (up to 90%), but at the same time high amount of chlorophyll was released (about 75%). In the pellet, 75% of the total starch was recovered in this zone.
- For higher *SI* values, most of the initial mass (60%) was recovered in the pellet. It produced higher starch recovery in the pellet than for low *SI* values, to the detriment of the starch purity. The protein yield in the supernatant decreased to the 50%, with a slight purity increase. The chlorophyll release in the supernatant decreased from 60% to 20%.

These results suggest the possibility to select the *SI* of the bead milling process as function of the main target product and the required purity. For example, if the target product is starch, the highlighted *SI* range should be selected for high starch recovery (80%) in the pellet and purity up to 20%. In this zone dry matter, proteins and pigments are mainly released in the supernatant (80% and 70% respectively) and are available for other biorefinery applications.

Otherwise, if the target metbolites are the soluble proteins with low level of chlorophyll associated, *SI* values higher than 10^{-4} J should be considered. In these conditions the recovery decreased to 50% but the supernatant was enriched up to 70–80% of proteins.

The use of small beads, corresponding to low *SI* values, resulted in an important miniaturization of the cell fragments and most of them remained in the supernatant after the centrifugation step.

The opposite trend was related to high *SI* values: the stress frequencies reduced the miniaturization of fragments, resulting in 60% recovery in the pellet during centrifugation. More starch was obviously recovered in the pellet, but together with all the insoluble components of the microalgae. The protein content recovered in the supernatant for high *SI* is reduced (50%). Safi et al. (2017) concluded that the maximum amount of protein released by bead milling represents 50% of the initial protein content of the biomass. We can suggest here that mainly cytoplasmic, water-soluble proteins were released for high *SI*, even if the 90% of cell disruption was reached. On the contrary, in low *SI* range, higher comminution was achieved and part of the non-soluble proteins was released and remained in the suspension after centrifugation.

As a conclusion, the optimization of the bead milling parameters cannot exclude the analysis of the product recovery in the following operation unit (in this case the centrifugation). The data reported highlighted that low *SI* did not correspond to mild disruption, while mild disruption could be considered for *SI* higher than the transition zone (in grey). In fact, high *SI* avoided miniaturization of the cell fragments but increased the energy consumption. Nevertheless, high

energy consumption in the disruption step, could be justified if it simplifies and save energy in the following steps for biomolecules separation (Safi et al., 2017; Montalescot PhD thesis).

The understanding of the different repartition of the product in function of the energy requirement for the disruption is a crucial point for the design of downstream process in function of the target product and the refinery application. It opens the way to a customization of the disruption parameters in function of the value and the required purity of the target product.

4. Conclusions

A kinetic model, including cell size distribution, was developed for *Chlorella sorokiniana* disruption in continuous bead miller. Glass beads of 0.4 mm size at impeller velocity of 14 $m.s^{-1}$ were the optimum conditions for efficient cell disruption. These conditions allowed disruption of big cells faster than small ones. A modified Stress Number, including cell diameter, was then proposed and validated.

Separation of starch, proteins and chlorophyll by mild centrifugation was studied according to disruption parameters. Optimal disruption conditions led to extreme comminution. An intermediate zone was pointed out for allowing moderate energy consumption and preserving efficient metabolites separation by centrifugation.

References

Angles, E., Jaouen, P., Pruvost, J., Marchal, L., 2017. Wet lipid extraction from the microalga Nannochloropsis sp.: disruption, physiological effects and solvent screening. Algal Res. 21, 27–34. https://doi.org/10.1016/j.algal.2016.11.005.

Asyraf Kassim, M., Aziz Rashid, M., Halim, R., 2017. In: Towards Biorefinery Production of Microalgal Biofuels and Bioproducts: Production of Acetic Acid from the Fermentation of Chlorella sp. and Tetraselmis suecica Hydrolysates, https://doi.org/10.4236/gsc.2017.72012.

Balasubramanian, S., Allen, J.D., Kanitkar, A., Boldor, D., 2011. Oil extraction from Scenedesmus obliquus using a continuous microwave system – design, optimization, and quality characterization. Bioresour. Technol. 102, 3396–3403. https://doi.org/10.1016/j.biortech.2010.09.119.

Becker, M., Kwade, A., Schwedes, J., 2001. Stress intensity in stirred media mills and its effect on specific energy requirement. Int. J. Miner. Process. 61, 189–208. https://doi.org/10.1016/S0301-7516(00)00037-5.

Beinert, S., Fragnière, G., Schilde, C., Kwade, A., 2015. Analysis and modelling of bead contacts in wet-operating stirred media and planetary ball mills with CFD–DEM simulations. Chem. Eng. Sci. 134, 648–662. https://doi.org/10.1016/j.ces.2015.05.063.

Blecher, L., Schwedes, J., 1996. Energy distribution and particle trajectories in a grinding chamber of a stirred ball mill. Comminution 44–45, 617–627. https://doi.org/10.1016/0301-7516(95)00070-4.

Chew, K.W., Yap, J.Y., Show, P.L., Suan, N.H., Juan, J.C., Ling, T.C., Lee, D.-J., Chang, J.-S., 2017. Microalgae biorefinery: high value products perspectives. Bioresour. Technol. 229, 53–62. https://doi.org/10.1016/j.biortech.2017.01.006.

Chisti, Y., 2008. Biodiesel from microalgae beats bioethanol. Trends Biotechnol. 26, 126–131. https://doi.org/10.1016/j.tibtech.2007.12.002.

Davis, R., Aden, A., Pienkos, P.T., 2011. Techno-economic analysis of autotrophic microalgae for fuel production. Spec. Issue Energy Algae Curr. Status Future Trends 88, 3524–3531. https://doi.org/10.1016/j.apenergy.2011.04.018.

de Winter, L., Klok, A.J., Cuaresma Franco, M., Barbosa, M.J., Wijffels, R.H., 2013. The synchronized cell cycle of Neochloris oleoabundans and its influence on biomass composition under constant light conditions. Algal Res. 2, 313–320. https://doi.org/10.1016/j.algal.2013.09.001.

Draaisma, R.B., Wijffels (Ellen), R.H., Slegers, P., Brentner, L.B., Roy, A., Barbosa, M.J., 2013. Food, commodities from microalgae. Food Biotechnol. Plant Biotechnol. 24, 169–177. https://doi.org/10.1016/j.copbio.2012.09.012.

Garrido, F., Banerjee, U., Chisti, Y., Moo-Young, M., 1994. Disruption of a recombinant yeast for the release of β-galactosidase. Bioseparation 4, 319–328.

Gifuni, I., Olivieri, G., Russo Krauss, I., D'Errico, G., Pollio, A., Marzocchella, A., 2017. Microalgae as new sources of starch: isolation and characterization of microalgal starch granules. Chem. Eng. Trans. 57. https://doi.org/10.3303/CET1757238.

Günerken, E., D'Hondt, E., Eppink, M.H.M., Garcia-Gonzalez, L., Elst, K., Wijffels, R.H., 2015. Cell disruption for microalgae biorefineries. Biotechnol. Adv. 33, 243–260. https://doi.org/10.1016/j.biotechadv.2015.01.008.

Kandilian, R., Soulies, A., Pruvost, J., Rousseau, B., Legrand, J., Pilon, L., 2016. Simple method for measuring the spectral absorption cross-section of microalgae. Chem. Eng. Sci. 146, 357–368. https://doi.org/10.1016/j.ces.2016.02.039.

Kula, M.-R., Schütte, H., 1987. Purification of proteins and the disruption of microbial cells. Biotechnol. Prog. 3, 31–42. https://doi.org/10.1002/btpr.5420030107.

Kwade, A., 1999a. Determination of the most important grinding mechanism in stirred media mills by calculating stress intensity and stress number. Powder Technol. 105, 382–388. https://doi.org/10.1016/S0032-5910(99)00162-X.

Kwade, A., 1999b. Wet comminution in stirred media mills? research and its practical application. Powder Technol. 105, 14–20. https://doi.org/10.1016/S0032-5910(99)00113-8.

Kwade, A., Schwedes, J., 2007. Chapter 6 Wet grinding in stirred media mills. In: Salman, Agba D., Michael, J.H. (Eds.), Handbook of Powder Technology. Elsevier Science B.V., pp. 251–382.

Kwade, A., Schwedes, J., 2002. Breaking characteristics of different materials and their effect on stress intensity and stress number in stirred media mills. Spec. Issue Honour Prof Jimbo 122, 109–121. https://doi.org/10.1016/S0032-5910(01)00406-5.

Molina Grima, E., Belarbi, E.-H., Acién Fernández, F., Robles Medina, A., Chisti, Y., 2003. Recovery of microalgal biomass and metabolites: process options and economics. Biotechnol. Adv. 20, 491–515. https://doi.org/10.1016/S0734-9750(02)00050-2.

Montalescot, V., Rinaldi, T., Touchard, R., Jubeau, S., Frappart, M., Jaouen, P., Bourseau, P., Marchal, L., 2015. Optimization of bead milling parameters for the cell disruption of microalgae: process modeling and application to Porphyridium cruentum and Nannochloropsis oculata. Bioresour. Technol. 196, 339–346. https://doi.org/10.1016/j.biortech.2015.07.075.

Moreno-Garcia, L., Adjallé, K., Barnabé, S., Raghavan, G.S.V., 2017. Microalgae biomass production for a biorefinery system: recent advances and the way towards sustainability. Renew. Sustain. Energy Rev. 76, 493–506. https://doi.org/10.1016/j.rser.2017.03.024.

Phong, W.N., Show, P.L., Ling, T.C., Juan, J.C., Ng, E.-P., Chang, J.-S., 2017. Mild cell disruption methods for bio-functional proteins recovery from microalgae—Recent developments and future perspectives. Algal Res. https://doi.org/10.1016/j.algal.2017.04.005.

Postma, P.R., Suarez-Garcia, E., Safi, C., Yonathan, K., Olivieri, G., Barbosa, M.J., Wijffels, R.H., Eppink, M.H.M., 2017. Energy efficient bead milling of microalgae: effect of bead size on disintegration and release of proteins and carbohydrates. Bioresour. Technol. 224, 670–679. https://doi.org/10.1016/j.biortech.2016.11.071.

Safi, C., Cabas Rodriguez, L., Mulder, W.J., Engelen-Smit, N., Spekking, W., van den Broek, L.A.M., Olivieri, G., Sijtsma, L., 2017. Energy consumption and water-soluble protein release by cell wall disruption of Nannochloropsis gaditana. Bioresour. Technol. 239, 204–210. https://doi.org/10.1016/j.biortech.2017.05.012.

Schwedes, J., Bunge, F., 1992. Comminution and transport behaviour in agitated ball mills. Adv. Powder Technol. 55–70.

Souliès, A., Pruvost, J., Legrand, J., Castelain, C., Burghelea, T., 2013. In: Rheological Properties of Suspensions of the Green Microalga Chlorella Vulgaris at various Volume Fractions, https://doi.org/10.1007/s00397-013-0700-z.

Van Vooren, G., Le Grand, F., Legrand, J., Cuiné, S., Peltier, G., Pruvost, J., 2012. Investigation of fatty acids accumulation in Nannochloropsis oculata for biodiesel application. Bioresour. Technol. 124, 421–432. https://doi.org/10.1016/j.biortech.2012.08.009.

Wijffels, R.H., Barbosa, M.J., Eppink, M.H.M., 2010. Microalgae for the production of bulk chemicals and biofuels. Biofuels Bioprod. Biorefin. 4, 287–295. https://doi.org/10.1002/bbb.215.